

**N 9 3 - 1 3 6 8 3****VISUALIZATION OF HYDROGEN INJECTION IN A SCRAMJET ENGINE  
BY SIMULTANEOUS PLIF IMAGING AND LASER HOLOGRAPHIC IMAGING**

**R.C. Anderson**  
National Aeronautics and Space Administration  
Lewis Research Center  
Cleveland, Ohio

**R.E. Trucco**  
General Applied Science Laboratories  
Ronkonkoma, New York

**L.F. Rubin and D.M. Swain**  
Rocketdyne, Rockwell International  
Canoga Park, California

**SUMMARY**

Flowfield characterization has been accomplished for several fuel injector configurations using simultaneous Planar Laser Induced Fluorescence (PLIF) and Laser Holographic Imaging (LHI). The experiments were carried out in the GASL-NASA HYPULSE real gas expansion tube facility, a pulsed facility with steady test times of about 350 $\mu$ sec. The tests were done at simulated Mach numbers 13.5 and 17.

The 2" x 1" rectangular cross-section scramjet model was tested with no fuel injection (a "tare" run), with hydrogen injection into N<sub>2</sub> (a "mixing" run) and with fuel injection into air or oxygen (a "combustion" run). These fuel injection experiments were done at fuel flow rates corresponding to equivalence ratios of 1, 2, and 3 in air. Three injector configurations were used: a 15° flush wall injector, a 10° wedge injector, and a 10° swept wedge injector. The model offered side-view flow visualization access through 1" x 12" fused silica side windows. The PLIF laser sheet was admitted through a 1" x 6" window in the top of the model. The facility test section windows used were 9" in diameter allowing a perpendicular view of the flow over a 9" length. A window in the top of the facility test section allowed optical access to the top window of the model.

Both single-shot PLIF images of hydroxyl radicals (OH) and LHI measurements were obtained during the combustion tests, with approximately 50 $\mu$ sec between the PLIF and LHI. Only the LHI techniques were applied to the mixing and tare experiments (no OH present). The OH PLIF images were produced by illuminating the flow with either a laser sheet parallel to the flow or with the sheet

cutting the flow at an angle to the direction of the freestream. The side-view LHI was used in the double-exposure infinite-fringe and finite-fringe interferometry mode. The resulting holograms are instantaneous snapshots of the flow integrated along the line of sight. The LHI system was also used in the 5  $\mu$ sec separation double-pulse interferometry mode in an attempt to reveal high frequency transient phenomena.

The PLIF system used a doubled Nd:YAG pumped dye laser tuned to 283 nm to excite the OH  $Q_1(7)$  line of the A-X(1,0) transition. The images from the 512x240 pixel CCD camera were spectrally filtered to avoid contamination from background emission and scattering. The 6" fused silica top window enabled the UV light sheet to probe the same region of the flow being simultaneously interrogated by the holographic imaging system.

The holographic recording system employed a 30 nsec. pulsed ruby laser. Reconstruction of the holograms was accomplished with a CW helium-neon laser after the tests.

Wall pressure and thin film heat flux gages and exit plane pitot pressure probes were used in addition to the PLIF and LHI measurements for all the scramjet tests. An OH emission/absorption apparatus based on an OH resonant lamp was also used during the combustion tests. These measurements were useful for comparing with quantified OH PLIF images and with CFD calculations. The OH measurement volume was located at the downstream end of the model. The OH emission/absorption apparatus and results are discussed in another paper.

The PLIF images reveal large-scale turbulence which is not readily seen in the line-of-sight integrated holographic interferograms, although the general flow field structures observed with the two techniques are quite consistent. In addition, wall heat flux measurements appear to correlate with the features evident in the holographic images.

## INTRODUCTION

Pulsed gas dynamic test facilities (e.g. shock and expansion tubes and tunnels) provide the only means for ground simulation of high Mach number flows. These tunnels typically have steady flow times measured in fractions of a millisecond<sup>1</sup>. The short test time presents unique measurement problems and it also motivates the researcher to use techniques providing as much information as possible from every test.

In addition the environment in the flowfield is usually hostile to intruding probes, and the small duct dimensions of typical test articles mean that intruding probes have an unacceptably large effect on the flow. Wall pressure and temperature measurements are nonintrusive but give little information about phenomena in the main flowfield. This main flowfield data is required to characterize boundary layer flow and to fully evaluate the fuel mixing processes.

Two and three dimensional optical measurement techniques are not intrusive and provide simultaneous measurement at many points within the flow. The information content of optical measurements is potentially extremely large. Furthermore, multiple and simultaneous multidimensional diagnostic measurements complement one another and provide better insight into flow phenomena than single measurements, especially for pulsed flow facilities.

Pulsed laser-based optical measurement techniques are particularly attractive for use in pulsed flow facilities, providing instantaneous snapshots of flowfield properties. Optical measurement techniques such as schlieren, shadowgraph, and holographic interferometry (LHI) yield visualization of density gradients in the flow. When, as in the present case, a combustor system is under investigation, measurement techniques which depend on species present in combustion can be used such as Planar Laser-Induced Fluorescence (PLIF) and OH emission/absorption.

The work reported herein marks the first time that several multidimensional measurements have been made simultaneously in a pulsed facility simulating Mach 13 and 17 flows with a test time between 300 and 400  $\mu$ sec. Several examples exist where a single multidimensional optical technique has been used in a shock tunnel. However, Mach numbers were generally lower and available test times were longer than those in the present work. Henckels et. al.<sup>2</sup> used infra-red scanning to measure the temperature field around a model in a shock tunnel at Mach 7.6 with a 5 ms test duration. Cassady and Lieberg<sup>3</sup> performed Planar Laser-Induced Fluorescence Temperature Measurements in a shock tunnel at Mach 9 with a 2 millisecond test time.

The focus of this paper is on the measurement technologies used and their application in a research facility. The following text briefly describes the HYPULSE facility, the models used for the experiments, and the setup for the LHI and PLIF measurements. Measurement challenges and solutions are discussed. Results are presented for experiments with several fuel injector configurations and several equivalence ratios. OH absorption measurements made during the same test series are discussed in another paper<sup>4</sup>.

## TEST FACILITY

The experiments described herein were carried out in NASA's HYPULSE facility at GASL. This is an expansion tube (6-inch tube diameter, 120ft overall length) which was originally constructed at NASA Langley Research Center in the 1960's for real gas aerothermal studies<sup>5</sup>. The tunnel was decommissioned in 1983, and eventually recommissioned as the NASA HYPULSE facility operated by General Applied Science Laboratories (GASL)<sup>6</sup>. The facility is presently located at GASL.

The expansion tube enjoys several advantages compared to other hypersonic test facilities. These are described in reference 7. One trade-off for these advantages is the test duration. HYPULSE

steady test time is typically in the 300 to 400 microsecond range, limiting the maximum allowable model length to about 3 ft (1 m).

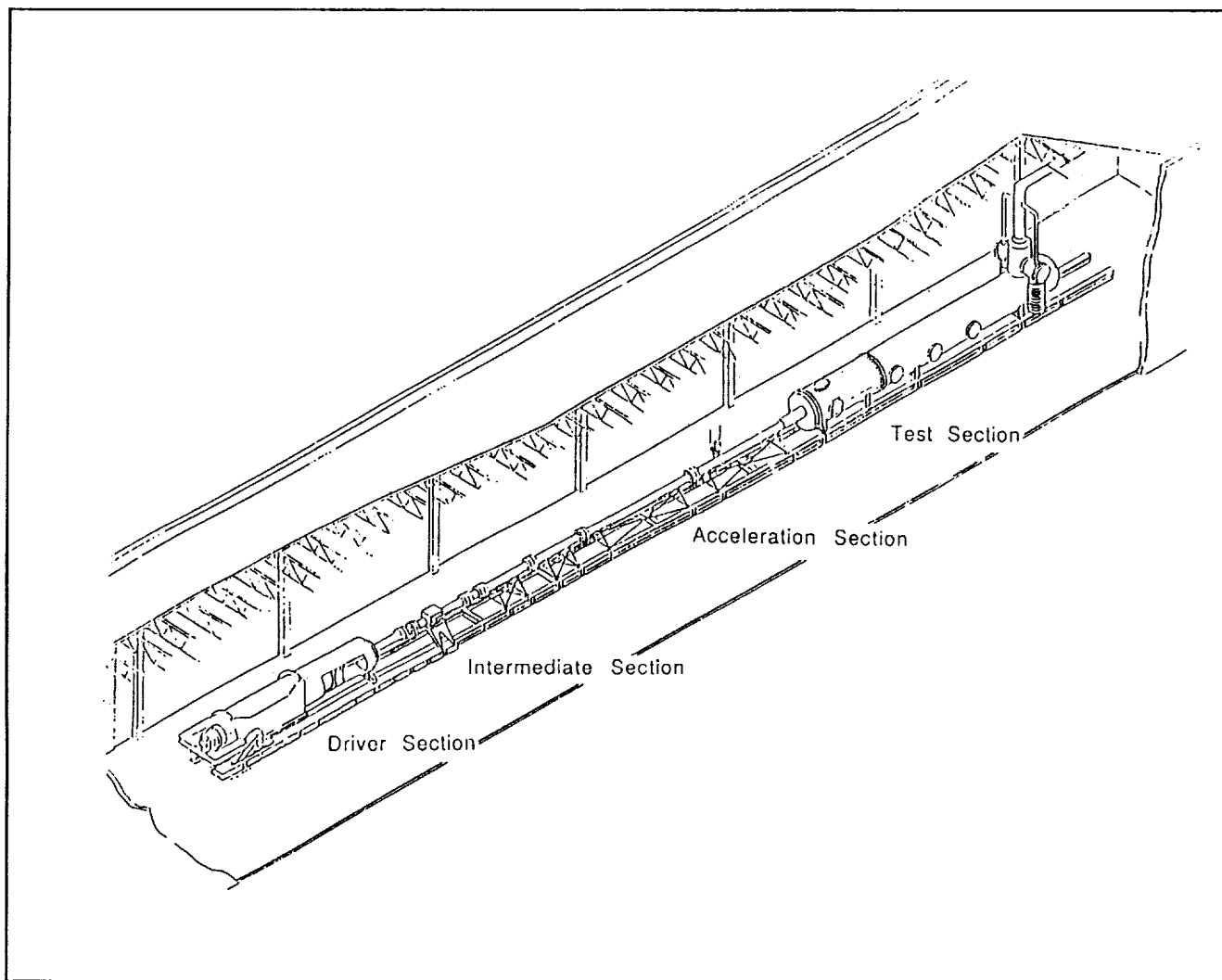


**Figure 1 - Isometric View of NASA HYPULSE Facility**

A schematic of the facility is shown in Figure 1. The facility consists of four sections: the driver section, the intermediate section, the acceleration section, and the test section/dump tank. The driver and intermediate sections are separated by a double metal diaphragm; and a mylar diaphragm separates the intermediate section and the acceleration/Test sections. The driver section is pressurized with helium and the short section between the metal diaphragms is pressurized to about half the pressure of the driver section. To start the flow the double diaphragm section is suddenly vented, bursting the diaphragms.

Facility transient data is acquired with a system composed of 80 transient waveform digitizers. Each digitizer can sample at a maximum rate of 1MHz with 12-bit voltage resolution and has on-board memory to store 512K samples. The data acquisition is controlled by a 386-based PC. This system is used to monitor facility operation and acquire pressure and heat flux data.

Piezoelectric pressure transducers provide pressure data and GASL-designed and manufactured heat flux gages provide heat flux data.

A Ludweig tube connected to a fast-acting valve (Trucco et al.<sup>8</sup>) was used to provide a gaseous hydrogen fuel supply for these experiments. The Ludweig tube fed a manifold connected to the injectors and was synchronized provide fuel before the test gas arrived at the test section.

Timing and triggering control were extremely important for the reasons detailed below. The sequence of events for a HYPULSE test run is given below in Table I.

TABLE I - TIMING OF HYPULSE FACILITY OPERATION EVENTS

Event	$t_{\text{test}} - t_{\text{event}}$	Event Duration
Evacuate Intermediate Section and Test Section/Dump Tank	- (1 hour)	45 min
Fill driver and between-diaphragms section; Fill Intermediate section to 28 mm Hg with Test GAS ( $N_2$ , Air, or $O_2$ ); Fill Test Section to 600 $\mu\text{m}$ Hg with helium.	- (45 min)	15 min
Begin vent of between-diaphragm section.	- (1-2 sec)	1-2 sec
Double diaphragm burst Mylar diaphragm burst	- 5 msec	
Fuel flow start	-2 msec	-

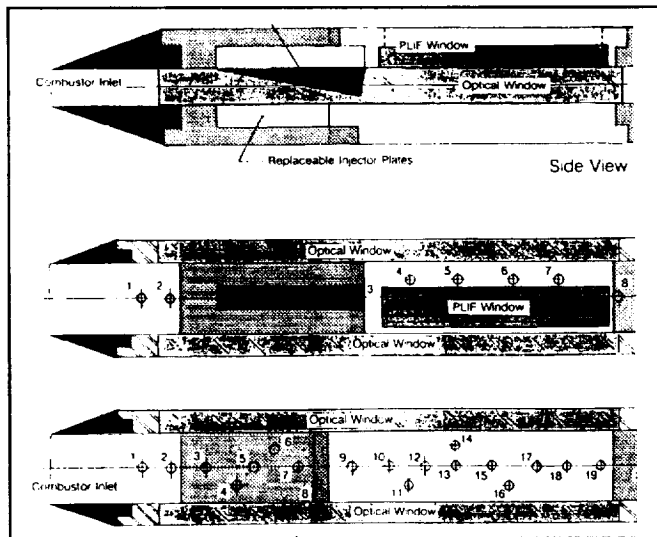


Figure 2 - Schematic of Unswept Ramp Injector Model.

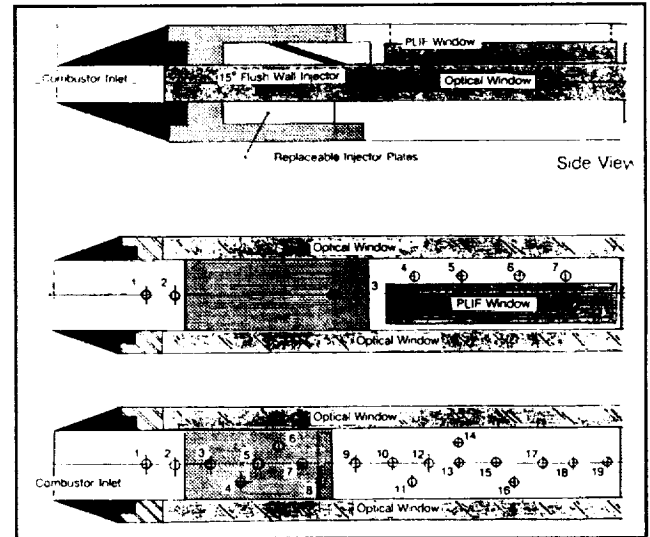


Figure 3 - Schematic of Flush Wall Injector Model

## TEST HARDWARE AND INSTRUMENTATION

### Model Hardware

Three injector configurations were tested during this program. Figures 2 through 4 show these configurations schematically. Figures 2-4 (top) show side views with the location and geometry of the injectors and optical windows. Figures 2-4 (middle) and (bottom) show the top and bottom views. Numbered holes shown in these views could be used for either pressure transducers or heat flux gages. The flow duct was rectangular in cross section with dimensions of 2 inches wide by 1 inch high. Optical access to the flow was available through three windows (top and both sides) in the Test Section/Dump Tank and three windows (also top and both sides) in the model. Window material was fused silica chosen for adequate transmission of wavelengths throughout the UV and visible spectrum. Since the test duration is so short heat transfer to the windows was low. Most of the diagnostic instrumentation components were housed in an air-conditioned enclosure just outside the Test Section/Dump Tank. Data acquisition equipment for other instrumentation was located in the facility control room.

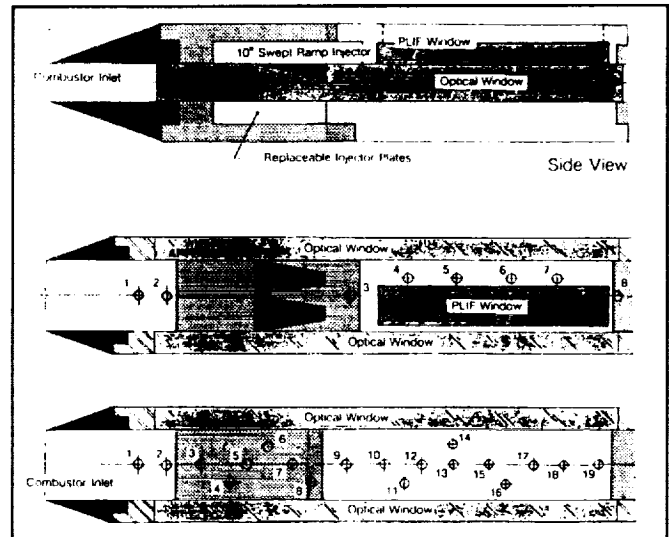
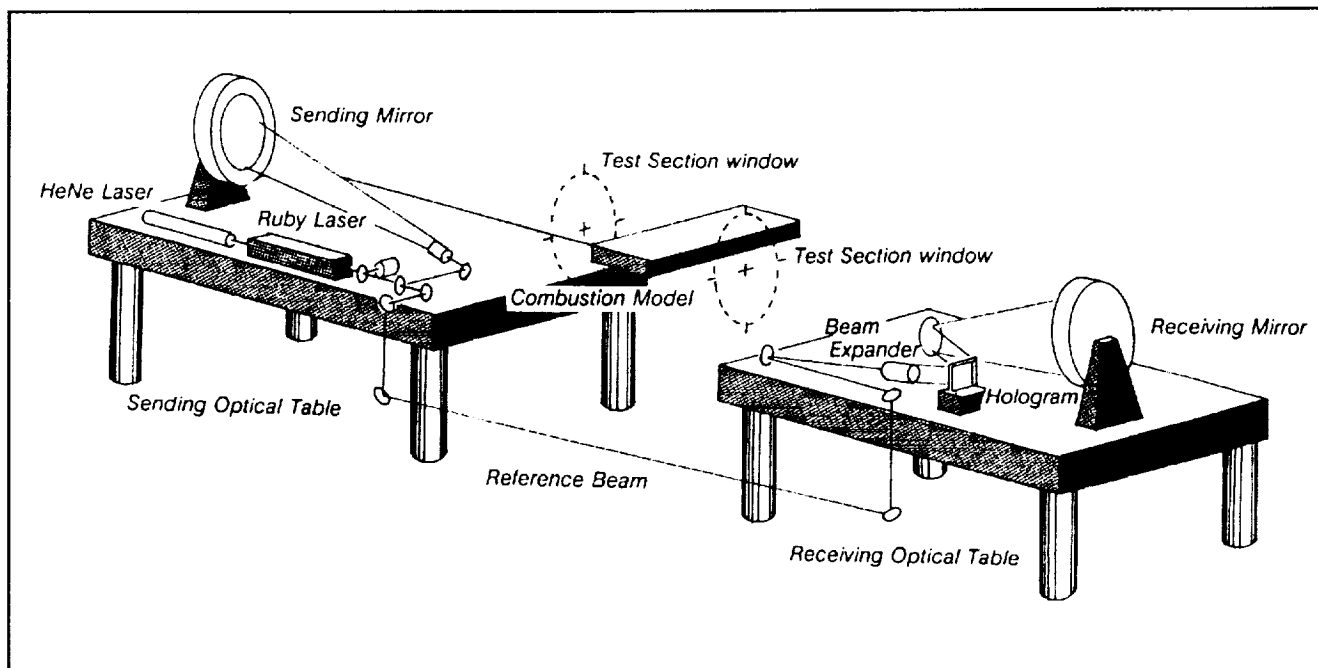


Figure 4 - Schematic of Swept Ramp Injector Model.

### Laser Holographic Interferometer

The Laser Holographic Imaging (LHI) system is shown in Figure 5. The system is mounted on two 4 x 10 foot vibration isolated tables (one on each side of the Test section) which were located in the enclosure mentioned above. For these tests some of the components for the PLIF and LHI systems occupied the same table. The test section is connected to the enclosure by 16 inch diameter rubber bellows which provide a light-tight environment.

A Q-switched ruby laser was used as the primary recording light source for the LHI system. Laser energy output was 30 milliJoules per 30 nsec pulse. A helium-neon laser was used for pre-test



**Figure 5 -** Diagram of Holographic Imaging System for HYPULSE.

alignment. A photodiode was used to confirm laser firing and synchronization. The main beam is split to form the object beam and the reference beam, at a 1 to 4 object to reference intensity ratio.

The reference beam is directed using several mirrors to pass around and outside the test section through a beam expander to the center of a photographic plate. The object beam is directed using parabolic mirrors through the test section to the center of the photographic plate. A shear-plate interferometer<sup>9</sup> is used to ensure that the reference beam and reconstruction beam are parallel. The reconstructed image was recorded on film. A helium-neon laser was used for hologram reconstruction.

### Planar Laser-Induced Fluorescence Measurement

A schematic of the PLIF system used is shown in figure 6. Not all of the system components shown were needed for the HYPULSE tests. The equipment used for these tests included the Neodymium:YAG-pumped dye laser system, two image detector systems, and the PC-based image acquisition and processing system. One detector is an intensified gated 512x240 pixel CCD camera; the other is an intensified 128 x 128 pixel diode array camera.

The YAG/dye laser beam was tuned to an electronic transition of the OH molecule near 283 nm using a propane torch to generate OH and a photomultiplier tube to monitor LIF. The beam was then directed to sheet-forming optics outside and above the Test section. The beam was formed into a sheet and split. Part of the beam was directed down through the Test section window through the

# MULTI-POINT, MULTI-PARAMETER DIAGNOSTIC SYSTEM

T-3366

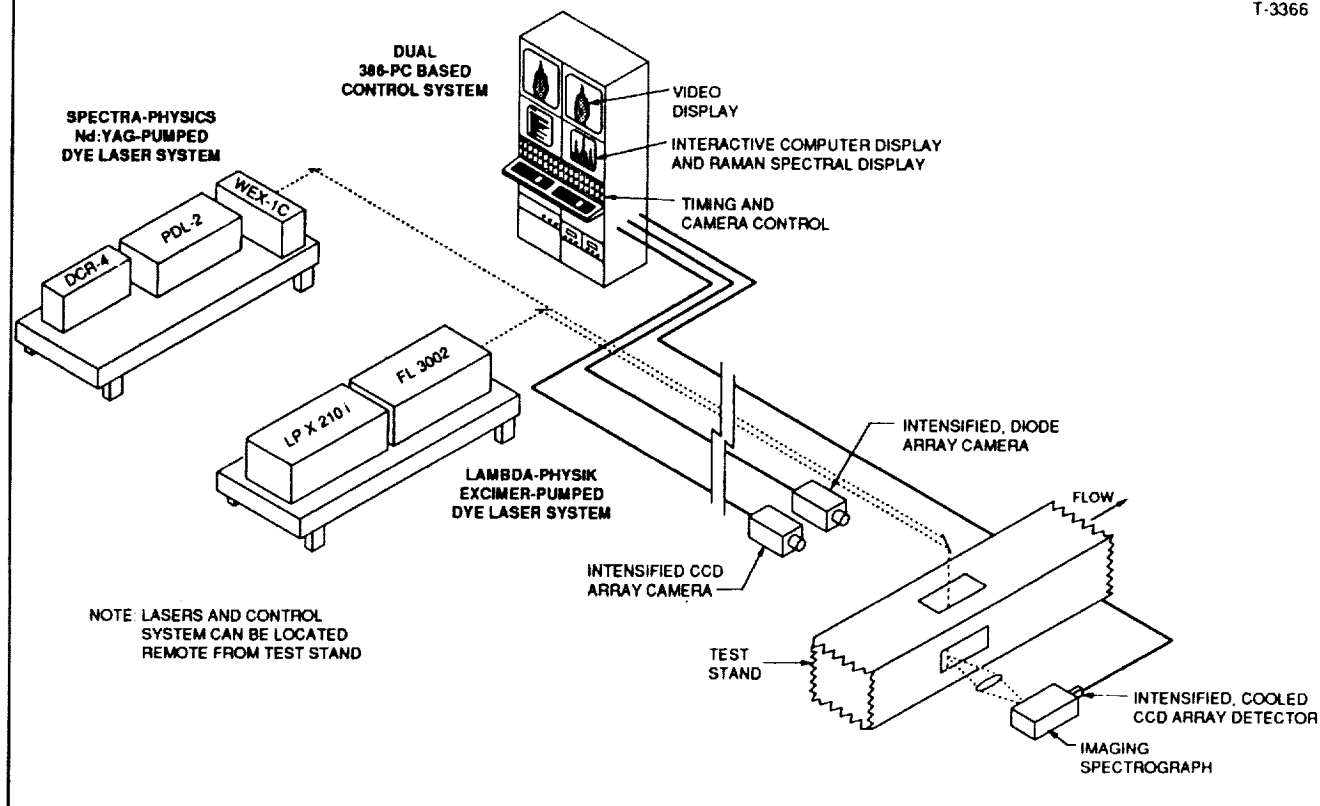


**Figure 6 - Schematic of Multipoint Multiparameter Diagnostic System.**

window on top of the model. The other part of the beam was directed to a fluorescent card. The beam image from the card was acquired by the 128x128 diode array camera system in real time during the test as a beam profile measurement. The effective beam profile was a weak but relatively significant function of the distance from the sheet-forming optics to the test article. To minimize any difference between the card-measured profile and the actual profile, the card was mounted the same distance from the sheet-forming optics as the test article probe volume.

The CCD camera was mounted at the side of the test section and was aimed through the Test section window to image the laser-induced fluorescence near 310 nm as viewed through the model window. Initially, a color filter was used to discriminate between the 283 nm laser wavelength and the OH fluorescence at 310 nm. In these tests, the color filter with its relatively broad passband did not sufficiently filter out the high background luminosity. To increase the spectral discrimination, an interference filter was installed with a much narrower passband centered on the OH emission wavelengths at 310 nm. This provided the necessary rejection characteristics.



As part of the pre-test activity, a fluorescent card was placed inside the model flow duct to assist in beam alignment. The 2D beam profile was acquired from the card using the 512 x 240 CCD camera system. Columns were summed and normalized in the two dimensional beamprofile images to yield the one dimensional beam profile used when available to correct PLIF images.

The PLIF system used was part of a larger Multiparameter Multipoint (MPMP) flow diagnostic system developed under a Rocketdyne contract with the NASA Lewis Research Center. The complete system includes an excimer-pumped dye laser system in addition to the components used for this test. To maximize fluorescence signal strength against the intense background emission expected, the Nd:YAG laser system was selected because of its higher pulse energy.

Use of the YAG-pumped dye laser presented severe timing and triggering challenges. This laser system requires a steady 10Hz pulse rate to maintain thermal stability and constant power supply charge per pulse. The laser pulse had to be timed to occur within the 350  $\mu$ sec test duration. This meant interrupting the laser for a period, and recharging and firing the laser in synchronization with the test period event.

Specialized circuitry was built to accomplish these timing requirements. If the delay was too long the pulse energy of the laser would decrease. A storage oscilloscope measuring the output of a photomultiplier was used to store the pulse shape during the test along with a typical undelayed pulse shape so that pulse decay could be measured. It was determined that a delay of 1 second or less was necessary to keep pulse strength at an acceptable level.

From the times in table 1 it can be seen that the double diaphragm venting occurs about 1-2 seconds before the test. This event was used to interrupt the laser. It was subsequently determined that interrupting the laser at vent start caused a delay that was too long and too variable. This resulted in laser pulse energy droop and jitter. An acceptable delay was created by interrupting the laser when the pressure in the between-diaphragm section fell below a pre-determined threshold rather than at vent start.

For both the LHI and PLIF laser systems the final trigger was derived from the output of pressure transducers sensing shock passage just upstream of the model. The LHI ruby laser was triggered at a slightly different time within the steady flow period to ensure that the PLIF camera intensifier was not gated ON during the ruby laser pulse.

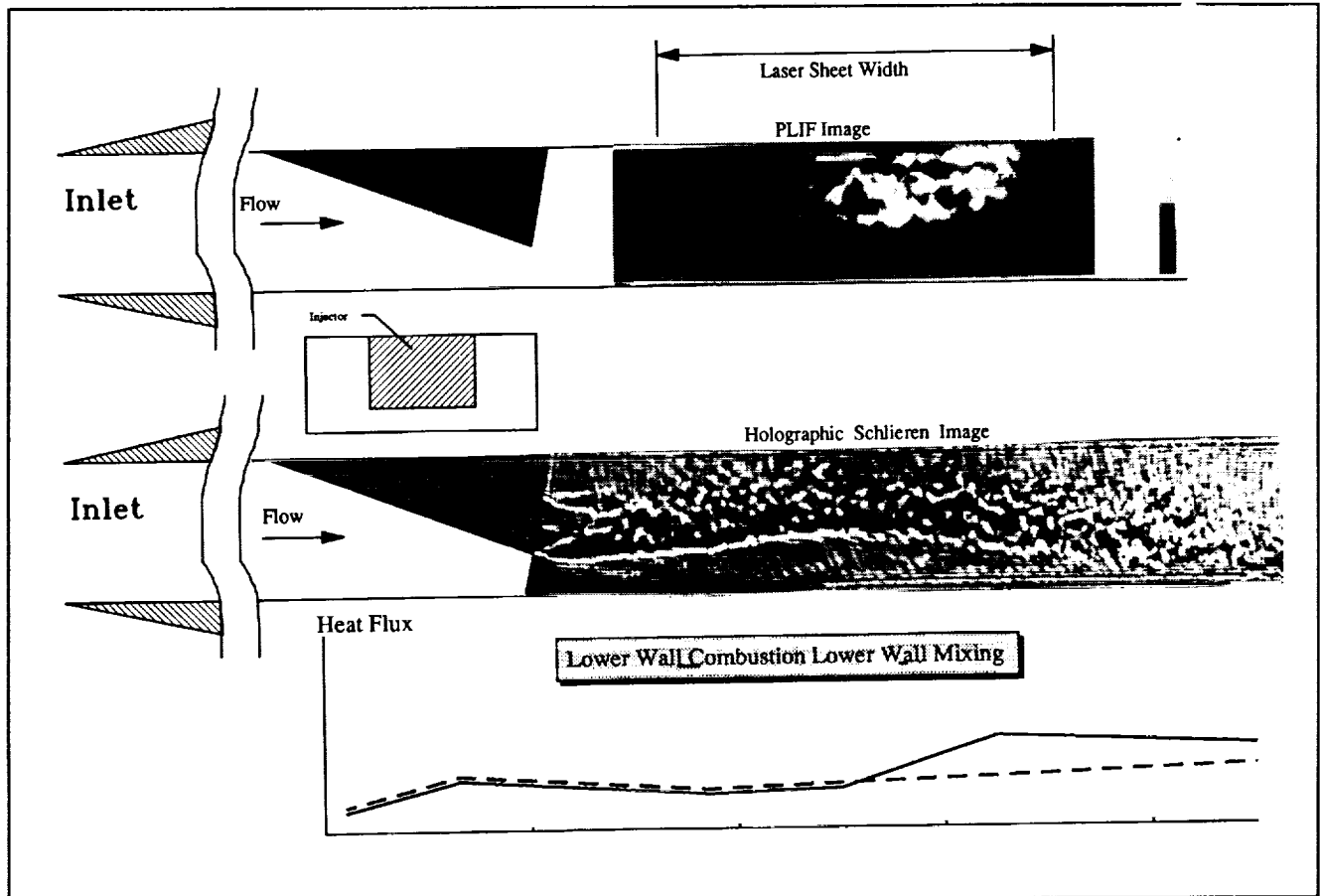


Figure 7 - HYPULSE Results For Unswept Ramp Injector Model  
Oxygen test gas;  $\Phi = 1.0$

## TEST RESULTS

### Unswept Ramp Injector

Figure 7 shows results from the PLIF, LHI and heat flux sensor measurements taken during tests using the unswept  $10^\circ$  ramp injector configuration. The PLIF laser sheet indicated at the top of figure 7 was directed through the top of the model to cut the flow in a plane in the center of the duct parallel to the flow. Two or three distinct flow structures are evident in the PLIF image which appear to correlate with the fuel streams evident in the hologram.

The holographic image shown in the middle of figure 7 was reconstructed as a schlieren image using a graded filter. The streams of gas leaving the injector ports are evident in the holographic image entering at the injector face and flowing from left to right. This hologram was not made at the same time as the PLIF image. It was made during a mixing experiment using nitrogen as the test gas.

The lower wall heat flux data plotted at the bottom of figure 7 compares the combustion test with a mixing test and appears to correlate with the PLIF and LHI data showing lower heat flux near the wall where there appears to be an expansion. Where the flow in the hologram appears to strike the wall the heat flux increases.

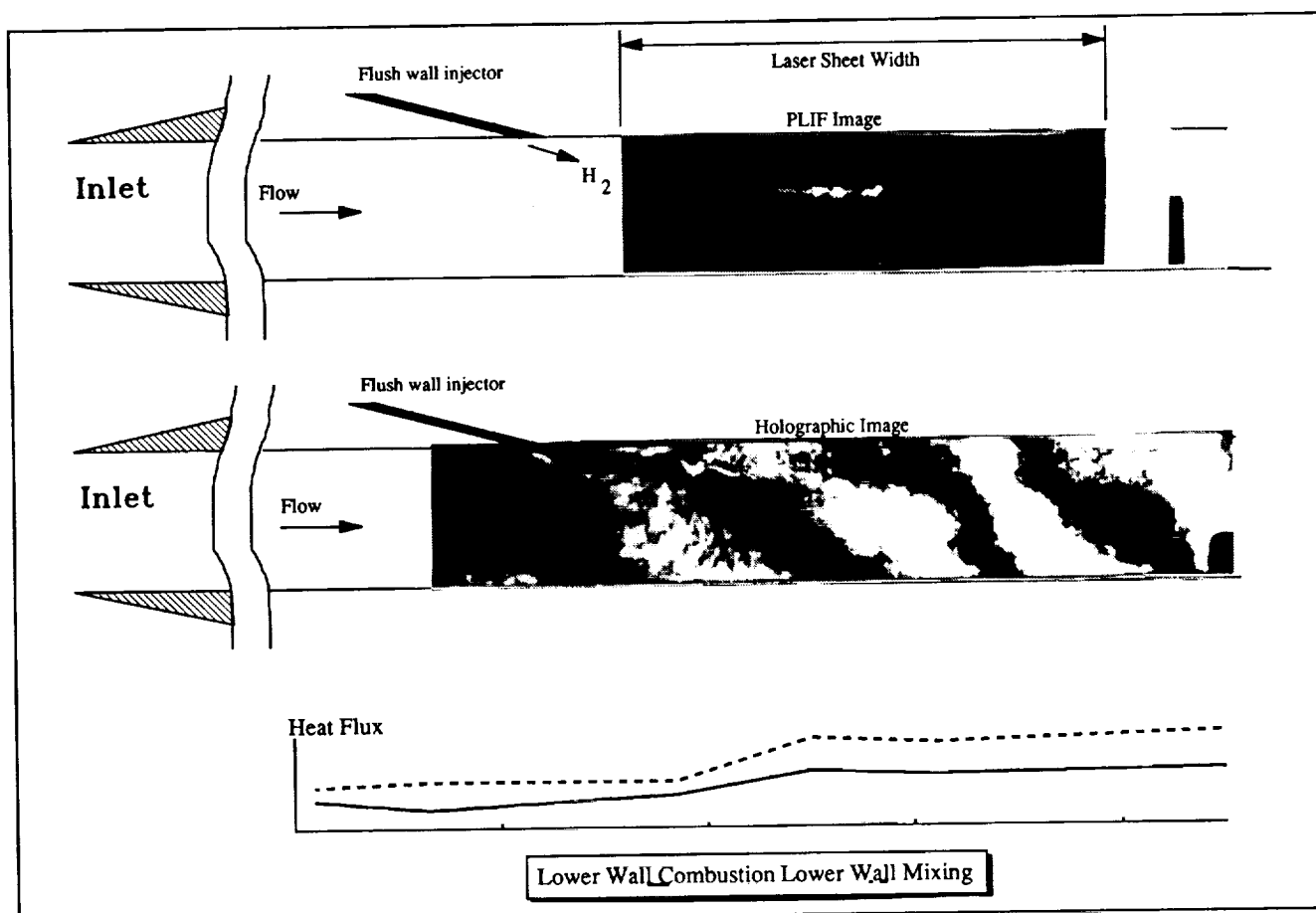


**Figure 8 - HYPULSE Results For Flush Wall Injector Model**  
Oxygen test gas;  $\Phi = 1.0$

#### Flush Wall Injector

Figures 8 and 9 show results from PLIF, LHI, and heat flux sensor measurements obtained during testing of the 15° flush wall injector model. The PLIF laser sheet shown at the top of figures 8 was

again directed through the top of the model to cut the flow in a plane in the center of the duct parallel to the flow. The holographic image shown in the middle of figure 8 has been reconstructed as an infinite fringe interferogram. The stream of fuel leaving the injector port is evident in the holographic image as it enters at the injector and flows from left to right. One straight and narrow reaction zone is evident in the PLIF image which appears to correlate with the fuel stream seen in the holographic image. The heat flux data seems to correlate with the other data showing a rise in the heat flux where the bow shock from the injected fuel hits the lower wall. The apparent increase in fluorescence along the lower wall in the PLIF image was determined to be emission.

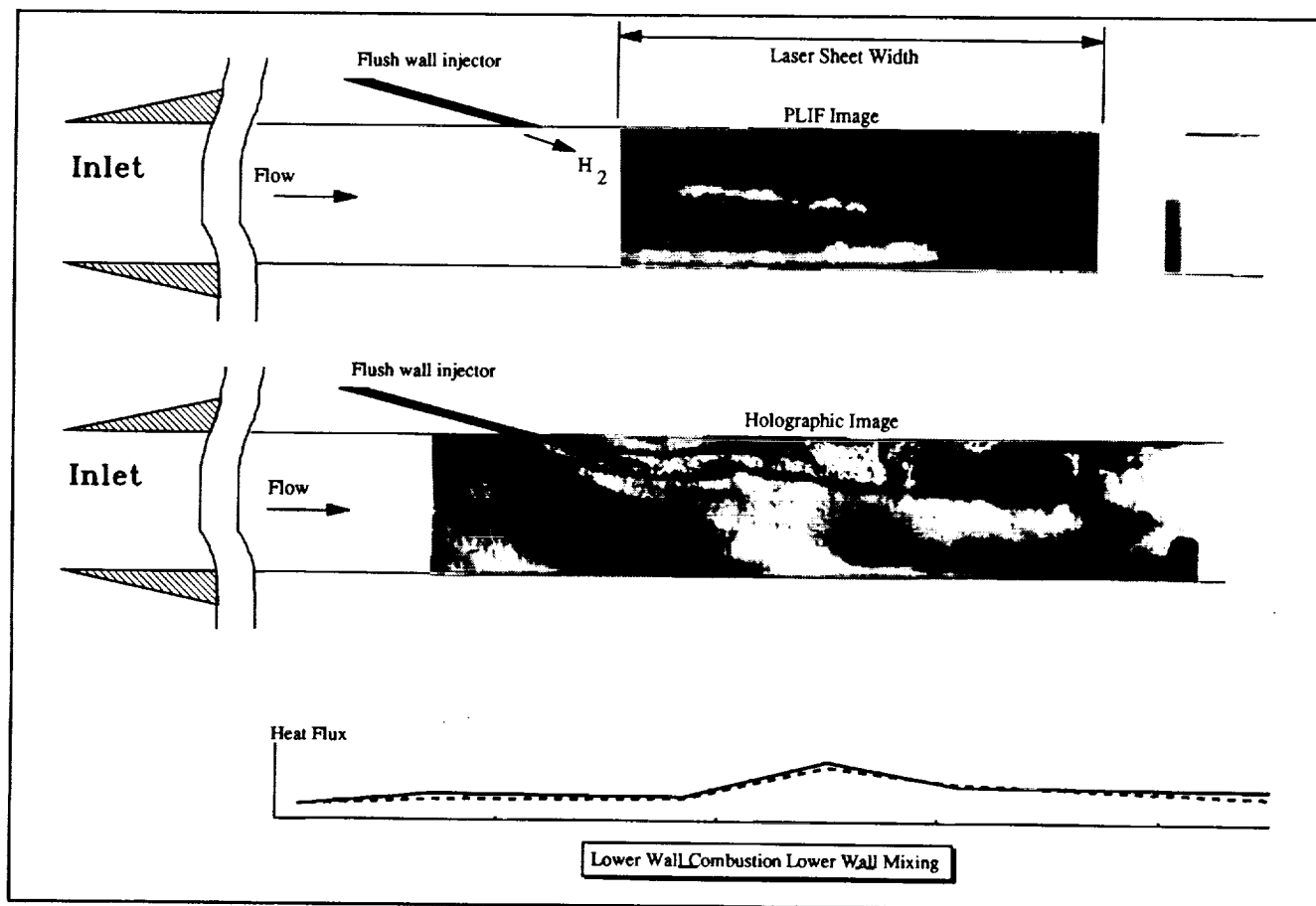


**Figure 9 - HYPULSE Results For Flush Wall Injector Model**  
Oxygen test gas;  $\Phi = 1.8$

Figure 9 shows flush wall injector results with a slightly higher equivalence ratio than that of figure 8. All other conditions are the same. The figure 9 PLIF image shows a structure similar to that of figure 8, but with the lower wall emission zone somewhat more evident.

The flush wall injector results are consistent with expectations. For low angle injection ( $15^\circ$ ), jet-induced longitudinal vortices are expected to be weak and self-entrainment small resulting in very limited spreading of the reaction zone. Furthermore, no significant distortion or enlargement of the mixing interface occurs.

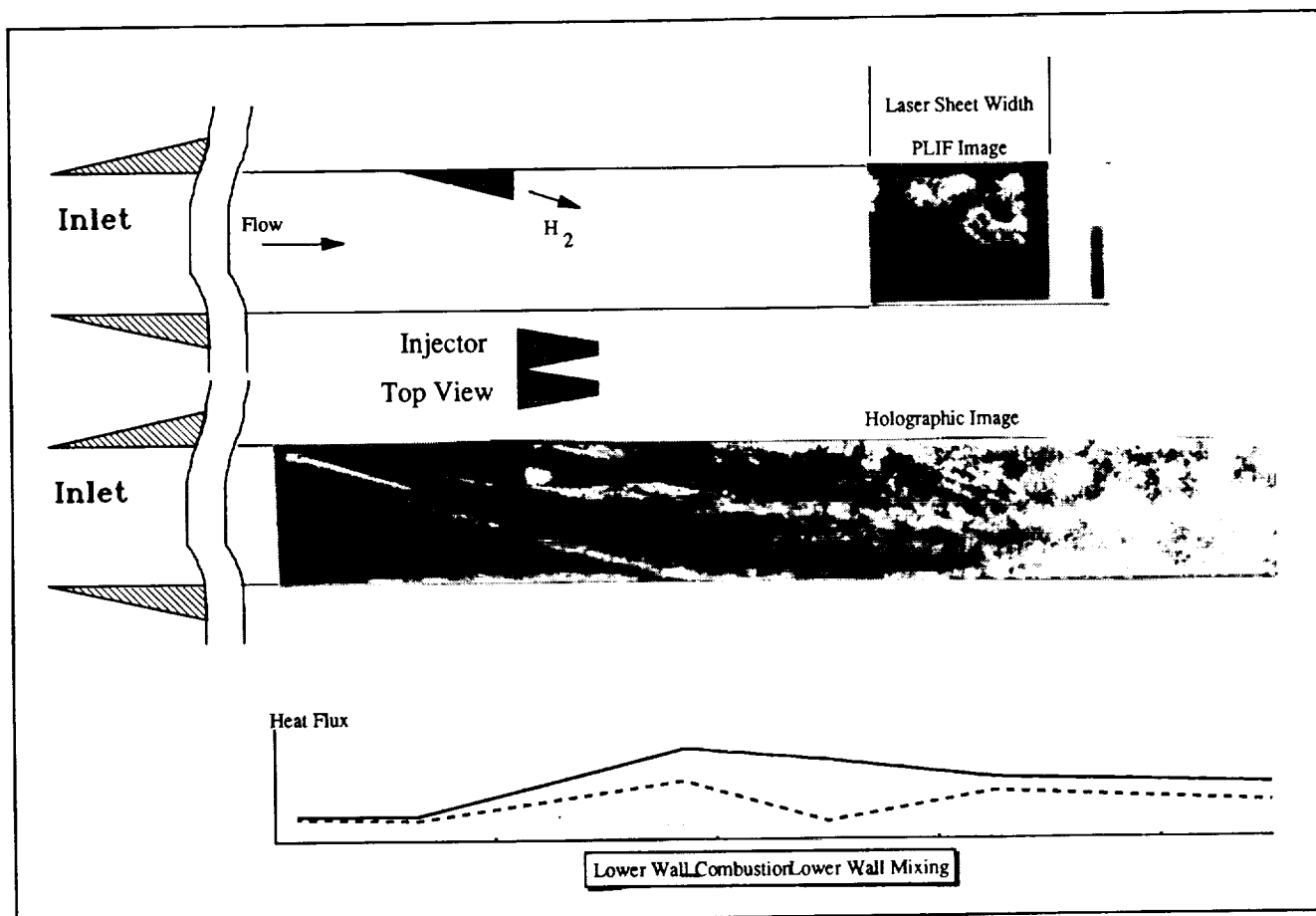


**Figure 10 - HYPULSE Results For Swept Ramp Injector Model**  
Oxygen test gas;  $\Phi = 1.0$

### Swept Ramp Injector

Figures 10 and 11 show results from PLIF, LHI, and heat flux sensor measurements obtained during testing of a dual  $10^\circ$  swept ramp injector model. For these tests the PLIF laser sheet again passed down through the flow but at a  $39^\circ$  angle to the flow direction rather than parallel. This was done to image OH distributions across the flow instead of along the flow. As a result the left side of the PLIF images in figures 10 and 11 corresponds to flow near the centerline of the duct; and the right side corresponds to flow near the far wall.

The holographic image shown in the middle of figure 10 has been reconstructed as an infinite fringe interferogram. The injector shadow and its bow shock are evident in the holographic image. The density perturbations caused by the stream of fuel leaving the injectors can be seen exiting the injector and flowing from left to right. The PLIF image indicates a reaction zone along the upper

wall. The interaction of the injectant stream with the ramp generated vortex pairs and the boundary layer appears to enhance the flow entrainment and small scale turbulence development.

The PLIF laser sheet was first sent through the model upstream of the location shown in Figure 10. Little or no signal was detected at that station. It was only when the laser sheet was moved downstream to the location shown that OH was detected. This indicates a significant delay in combustion onset.

The lower wall heat flux data in figure 10 again shows the expected increase due to the injector bow shock striking the wall.

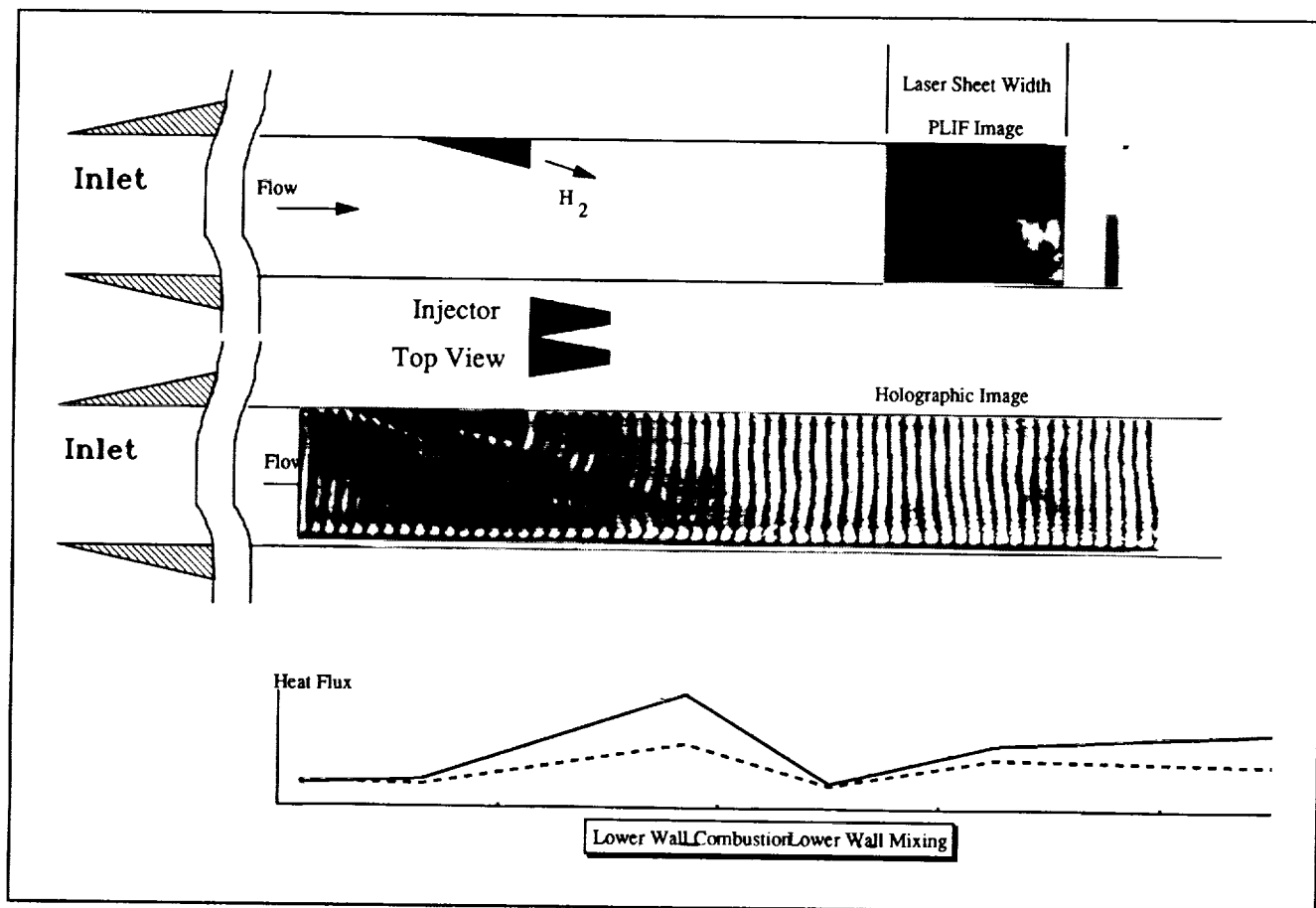


**Figure 11 - HYPULSE Results For Swept Ramp Injector Model**  
Oxygen test gas;  $\Phi = 3$ .

Figure 11 shows swept ramp data for an equivalence ratio of 3. The hologram image in this case is a finite fringe interferogram. Fringes are created by displacement of the holographic plate after the first exposure and variations in the flow density manifest themselves as perturbations of the fringes.

The reaction zone for the figure 11 test has clearly shifted toward the lower wall. Since the equivalence ratio is proportional to injectant dynamic pressure this shifting of reaction zone may be interpreted as the effect of increased jet penetration. It is also possible that the reaction zone could

have shifted downstream. There is some indication that at this high equivalence ratio, excess hydrogen fuel may have a reaction quenching effect which would increase ignition delay.

### Data Processing

Visual representation of the holographic images is relatively straightforward simply involving photographing the reconstructed image. PLIF image processing is more complex. In addition to the qualitative information presented in figures 7-11 estimates were made of the OH concentration for each of the PLIF images. These estimates were determined by a two step process. First the absolute fluorescence intensity was determined and then this intensity was related to the absolute number density of OH.

The absolute fluorescence intensity for each image was determined using camera calibration factors. The absolute photon count in the image in a given pixel may be written as a function of the total probed species number density and spectroscopic and geometric parameters. Detailed analysis of flowfield properties was beyond the scope of the work given resource constraints so rough estimates of fluorescence yield were made based on estimates of spatially averaged flowfield conditions in the locations probed by the PLIF sheet. The number density estimates for maximum OH concentration fell generally within the low to mid  $10^{15} \text{ cm}^{-3}$  range.

### CONCLUDING REMARKS

Simultaneous use of PLIF and LHI techniques has been demonstrated for several hypersonic injector configurations in the NASA HYPULSE facility. Unique challenges presented by the extremely short test duration and the required simultaneous operation of two pulsed laser systems were met successfully.

The combination of gated intensified cameras and narrow spectral filtering provided the capability for PLIF imaging of low OH concentrations in the flow. PLIF Data was acquired in both longitudinal and crossflow planes.

Simultaneous use of the LHI and PLIF systems was advantageous and permitted correlations to be made between density gradients and combustion zones.

## REFERENCES

1. Harsha, P.; Waldman, B.: "The NASP Challenge: Testing for Validation," First National Aero-Space Plane Conference, AIAA 89-5005, 1989.
2. Henckels, A.; Maurer, F.; Olivier, H.; Gronig, H.: "Fast Temperature Measurement by Infra-red Line Scanning in a Hypersonic Shock Tunnel", *Experiments in Fluids*, vol. 9, pp 298-300, 1990.
3. Cassady, P.E.; Lieberg, S.F.: "Planar Laser Induced Fluorescence Measurements in Hypersonic Air Flowfields", AIAA 91-1492, 1991.
4. Lempert, W.R.; Trucco, R.E.: "Resonance Lamp Absorption Measurement of OH Number Density and Temperature In Expansion Tube Scramjet Engine Tests", *NASA Langley Measurement Technology Conference*, NASA CP-3161, 1992.
5. Miller, C.G.; Jones, J.J.: "Development and Performance of the NASA Langley Research Center Expansion Tube/Tunnel, A Hypersonic Hypervelocity Real Gas Facility", *Proc. 14th Int'l. Symp. Shock Tubes and Waves*, Sydney, Australia, 1983.
6. Tamagno, J.; Bakos, R.; Pulsonetti, M.; Erdos, J.: "Hypervelocity Real Gas Capabilities of GASL's Expansion Tube (HYPULSE) Facility," AIAA 90-1390, 1990.
7. Erdos, J.; Tamagno, J.; R. Bakos, R.; Trucco, R.: "Experiments on Shear Layer Mixing at Hypervelocity Conditions", *30th Aerospace Sciences Meeting*, AIAA 92-0628, 1992.
8. Trucco, R.; Danziger L.: "Performance of a Fast Acting Valve for Hydrogen Injection into a Scramjet Engine Model", GASL TM 232, 1989.
9. Steel, W.H.: *Interferometry*, Cambridge University Press, London, 1967.